ChemComm

Accepted Manuscript

This article can be cited before page numbers have been issued, to do this please use: D. Sheet, S. Bhattacharya and T. K. Paine, *Chem. Commun.*, 2015, DOI: 10.1039/C5CC01652E.

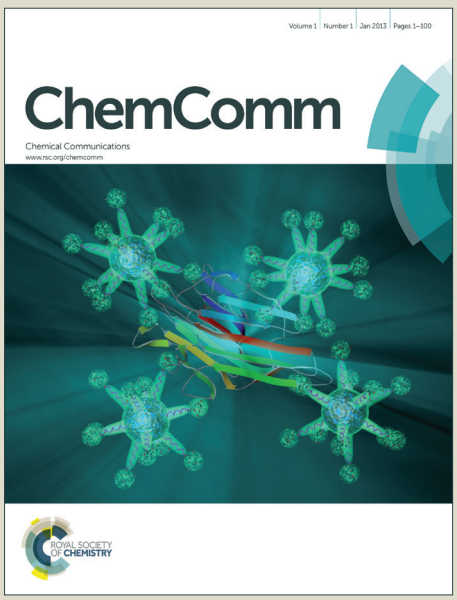

ROYAL SOCIETY OF CHEMISTRY

www.rsc.org/chemcomm

Dynamic Article Links ▶
View Article Online
DOI: 10.1039/C5CC01652E

Cite this: DOI: 10.1039/coxx00000x

www.rsc.org/xxxxxx

ARTICLE TYPE

Dioxygen Activation and Two Consecutive Oxidative Decarboxylations of Phenylpyruvate by Nonheme Iron(II) Complexes: Functional Models of Hydroxymandelate Synthase (HMS) and CloR**

Debobrata Sheet,[a] Shrabanti Bhattacharya [a] and Tapan Kanti Paine [a]*

Received (in XXX, XXX) Xth XXXXXXXXX 20XX, Accepted Xth XXXXXXXXX 20XX
DOI: 10.1039/b000000x

Two mononuclear iron(II)-phenylpyruvate complexes of monoanionic facial N_3 ligands are reported to react with dioxygen to undergo two consecutive oxidative decarboxylation steps via an iron-mandelate complex mimicking the function of HMS and CloR.

Alpha-keto acid-dependent oxygenases constitute a large superfamily of nonheme iron enzymes that couple the oxidative decarboxylation of the α-keto acid cofactors concomitant with the oxidation of substrates.[1-4] Hydroxymandelate synthase (HMS) and 4-hydroxyphenylpyruvate dioxygenase (HPPD) belong to the same superfamily of α-keto acid dependent enzymes.[5-9] HMS is involved in the first step of the biosynthesis of *p*-hydroxyphenylglycine, a nonproteiogenic amino acid component of antibiotics such as vancomycin.[6, 10] HMS, expressed from a calcium dependent antibiotic (CDA) *Amycolatopsis orientalis*, catalyzes the chiral oxidation of 4-hydroxyphenylpyruvate (4HPP) to (*S*)-4-hydroxymandelate (4HMA) (Scheme 1a).[7, 10-12] The structure of cobalt(II) substituted HMS was solved with the product hydroxymandelate coordinated to the metal center in a bidentate fashion.[7] HMS exhibits high structural similarity to that of HPPD, an evolutionary related enzyme that catalyzes the second step of the tyrosine catabolism pathway.[7, 13] HPPD and HMS are the exceptions in the α-keto acid-dependent enzymes as both the enzymes use a common substrate 4-hydroxyphenylpyruvate (4HPP).[5] The common goal is to hydroxylate 4HPP with the incorporation of both the atoms of O_2 into the substrate (Scheme 1a). These enzymes follow the mechanism typical of α-keto acid-dependent dioxygenases. An iron(IV)-oxo intermediate,[14] generated in the reaction with O_2, hydroxylates the substrate 4HPP. In the case of HMS, the iron(IV)-oxo abstracts an α-H atom from 4-hydroxyphenylacetate intermediate and hydroxylates the benzylic carbon via OH rebound mechanism affording hydroxymandelate (4HMA).[6, 7, 15, 16] In HPPD, on the other hand, spatial orientation of the substrate (4HPP) and steric factors controls the regiospecific delivery of the oxo atom from the iron(IV)-oxo oxidant.[5, 17]

Another functionally related bifunctional nonheme iron oxygenase CloR is involved in the biosynthesis of aminocoumarin antibiotics such as chlorobiocin.[18] These antibiotics contain a 3-dimethylallyl-4-hydroxybenzoate (3DMA-4HB) moiety whose formation from 3-dimethylallyl-4-hydroxyphenylpyruvate (3DMA-4HPP) is catalyzed by CloR via the formation of 3-dimethylallyl-4-hydroxymandelic acid (3DMA-4HMA) (Scheme 1b).[18] CloR does not have sequence similarity to any known oxygenases. However, HMS and CloR are similar in terms of reactivity and are involved in benzylic hydroxylation. The enzyme CloR uses 3DMA-4HPP (in the first step of the reaction) whereas HMS uses 4HPP as substrate/α-keto acid cofactor.

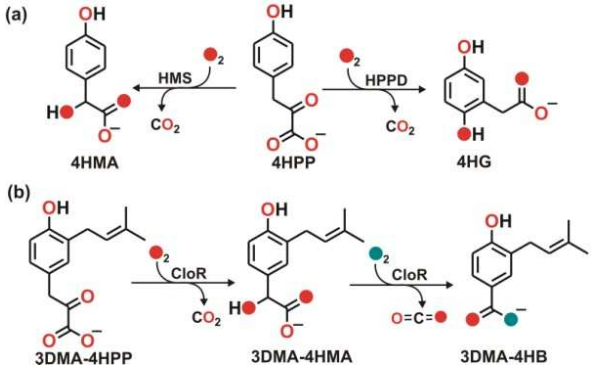

Scheme 1 Reactions catalyzed by (a) HMS and HPPD, and by (b) CloR.

In biomimetic chemistry, a large number of functional models for α-keto acid-dependent oxygenases have been reported.[4, 19-21] We have recently reported a functional model for the second step of CloR.[22] While some progress has been made in understanding the decarboxylation/oxidative C-C bond cleavage mechanism of phenylpyruvic acid by iron complexes of polydentate ligands,[23, 24] there is no nonheme iron(II)-phenylpyruvate complex mimicking the function of HMS or both the steps catalyzed by CloR. Since monoanionic facial tris(pyrazolyl)borate ligands (Tp) have widely been used to develop models for nonheme iron oxygenases,[4, 19, 21, 25-28] we have investigated the iron(II)-phenylpyruvate chemistry of different Tp ligands. As an outcome of our investigation, we report herein the synthesis and characterization of two nonheme mononuclear iron(II) complexes, $[(Tp^{Ph,Me})Fe^{II}(PPH)]$ (**1**) and $[(Tp^{Me2})Fe^{II}(PPH)]$ (**1a**), where $Tp^{Ph,Me}$ = hydrotris(3-phenyl-5-methylpyrazolyl)borate, Tp^{Me2} = hydrotris(3,5-dimethylpyrazolyl)borate, and PPH is monoanionic phenylpyruvate (Fig. 1). The phenylpyruvate complexes react with O_2 to undergo oxidative decarboxylation and concomitant hydroxylation of the benzylic carbon of phenylacetic acid resulting in the formation of iron(II)-mandelate complexes. The

View Article Online
DOI: 10.1039/C5CC01652E

latter further activates O_2 to undergo oxidative decarboxylation. The reactivity of the iron(II)-PPH complexes toward O_2 and the mechanism of two consecutive oxidative decarboxylations of phenylpyruvate is reported in this communication.

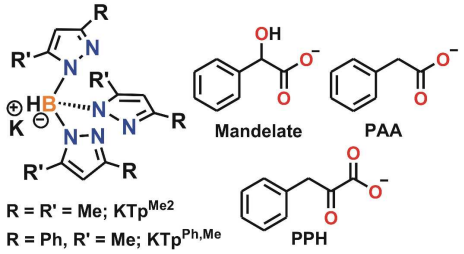

Fig. 1 Ligands and model substrates.

The iron(II)-α-keto acid complexes (**1** and **1a**) were synthesized by mixing equimolar amounts of the respective Tp ligand, $FeCl_2$ and NaPPH in dichloromethane-methanol solvent mixture (Experimental Section, ESI). The ESI-mass spectra of **1** and **1a** exhibit molecular ion peaks at *m/z* = 703.03 and 516.06 with the isotope distribution patterns calculated for [**1**+H^+] and [**1a**]$^+$, respectively (Figs. S1 and S2, ESI). The complexes display paramagnetically shifted ^{1}H NMR spectra in CD_3CN indicating high-spin nature of the iron(II) centers (Figs. S3 and S4, ESI). The optical spectrum of complex **1** in acetonitrile shows broad bands at around 422 and 552 nm, in which the latter peak arises due to the iron(II)-to-keto metal to ligand charge transfer transition (MLCT). The MLCT bands suggest a bidentate chelation of the α-keto acid (PPH) to the iron(II) centers via one keto oxygen and one carboxylate oxygen in solution. For complex **1a**, the MLCT bands are shifted to 413 and 560 nm. Similar MLCT bands with low extinction coefficients (~1000 $M^{-1}cm^{-1}$) have been observed in previously reported iron(II)-α-keto acid complexes of hydrotris(3,5-diphenylpyrazolyl)borate) (Tp^{Ph2}) ligand.[20, 23]

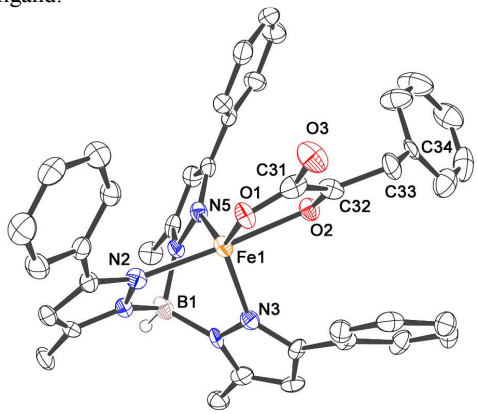

Fig. 2 ORTEP plot of [($Tp^{Ph,Me}$)Fe^{II}(PPH)] (**1**). All the hydrogen atoms except for B1 have been omitted for clarity.

The single crystal X-ray structure of **1** reveals a five-coordinate mononuclear complex where the iron center is coordinated by three pyrazole nitrogens from the $Tp^{Ph,Me}$ ligand, and one carbonyl oxygen (O2) and one carboxylate oxygen (O1) atom of a monoanionic phenylpyruvate (Fig. 2). Similar binding mode of keto acid is observed in the reported five-coordinate iron(II)-α-keto acid complexes of Tp^{Ph2} ligand.[20, 23] The average iron(II)-N(pyrazole) bond length is typical of high-spin iron(II) complexes.[20, 23] The iron center resides in a distorted trigonal bipyramidal coordination geometry (τ = 0.57),[29] where the trigonal plane is formed by the pyrazole nitrogens N5 and N3, and the carboxylate O1. The axial positions are occupied by the pyrazole nitrogen (N2) and the keto oxygen (O2) with the N2–Fe1–O2 angle of 174.3(2)° (Table S1). The Fe1–O2 bond distances of 2.258(6) Å and C31–C32 of 1.555(12) Å clearly indicates that PPH does not enolize upon binding with iron(II) center.[23, 24] Although single crystals of complex **1a** could not be isolated, the spectroscopic data indicate a very similar binding mode of PPH as in **1**.

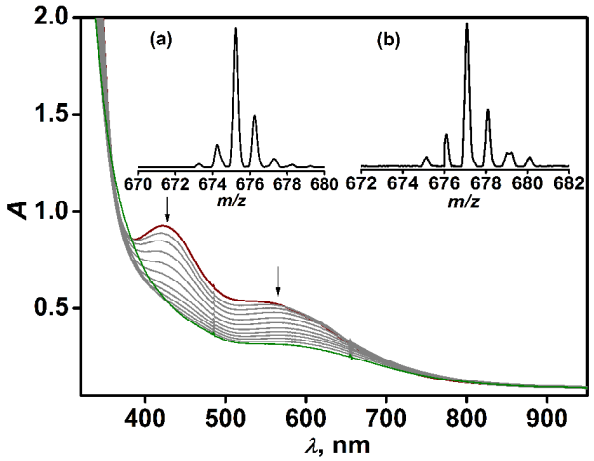

Fig. 3 Optical spectral changes during the reaction of **1** (1 mM) with dioxygen in acetonitrile at 295 K. Inset: ESI-mass spectra (positive ion mode, acetonitrile) of the oxidized solution after the reaction of **1** with (a) $^{16}O_2$ and with (b) $^{18}O_2$ in acetonitrile for 10 min.

The red solution of complex **1** in acetonitrile rapidly changes to green upon reaction with O_2 over a period of 1h during which the CT bands at 422 and 552 nm gradually decays (Fig. 3). The ESI-mass spectrum of the oxidized solution displays an ion peak at *m/z* = 675.2 with the isotope distribution pattern for [{($Tp^{Ph,Me}$)Fe^{II}(PAA)}+H^+] (PAA = phenylacetate) which is shifted two mass units higher to *m/z* = 677.2 after reaction with $^{18}O_2$, indicating incorporation (>95%) of one oxygen atom from dioxygen into the decarboxylated product (PAA) (Fig. 3, Inset). Complex **1a** takes about 1 h for complete decay of the CT bands and the ESI-mass spectrum of the oxidized solution suggests the formation of [(Tp^{Me2})Fe^{II}(PAA)] (Figs. S5 and S6, ESI).

Time-dependent ^{1}H NMR studies (Fig. S7, ESI) in CD_3CN reveal the formation of benzaldehyde and the ^{1}H NMR spectrum of the final oxidized solution bears resemblance to that of an independently isolated complex [($Tp^{Ph,Me}$)Fe^{II}(PAA)] (**2**) (Fig. S7 and Experimental Section, ESI). Further, the GC-mass spectra reveal the formation of phenylacetic acid, benzoic acid and benzaldehyde with the ion peaks at *m/z* = 136, 122 and 106, respectively (Figs. S8 and S9, ESI). With $^{18}O_2$, the phenylacetic acid peak is shifted to *m/z* = 138 while that of benzaldehyde is shifted to *m/z* =108 with (50% ^{18}O). The ion peak of benzoic acid, on the other hand, is shifted two and four mass unit to *m/z* = 124 (25% ^{18}O) and 126 (70% ^{18}O) (Figs. S8 and S9, ESI). GC-MS of the methyl ester derivatives of phenylacetic acid and benzoic acid also confirm the incorporation of labeled oxygen (Fig. S10, ESI). The labeling experiment data unambiguously establish that while one oxygen atom from O_2 is incorporated each into phenylacetic acid and benzaldehyde, two oxygen atoms from O_2 are

View Article Online
DOI: 10.1039/C5CC01652E

incorporated into benzoic acid. In addition to phenylacetic acid, the formation of benzaldehyde and benzoic acid from phenylpyruvic acid is intriguing. Of note, the reported iron(II)-PPH complex [(Tp^{Ph2})Fe^{II}(PPH)] undergoes oxidative decarboxylation to form phenylacetic acid as the only product.[23] Analysis of organic products from **1** through time-dependent ^{1}H NMR spectroscopy reveals that in addition to phenylacetic acid, the amounts of benzaldehyde and benzoic acid steadily increase with time. Between 10-20 min, a new peak at 5.24 ppm, attributable to mandelic acid, is observed which subsequently decays (Fig. S11, ESI). Mandelic acid therefore forms as an intermediate product which does not accumulate in a large amount. Finally, at the end of the reaction a product distribution of phenylacetic acid (58%), benzaldehyde (33%), and benzoic acid (8%) is observed. Complex **1a**, after reaction with O_2, affords phenylacetic acid (77%), benzaldehyde (5%), benzoic acid (4%), and mandelic acid (3%). In the reaction, about 8-10% phenylpyruvic acid remains unreacted (Fig. S12, ESI). While the iron-mandelate complex from **1** could not be observed in the ESI-mass spectrum, the final oxidized solution of **1a** exhibits a small ion peak at *m/z* = 504.2 with the isotope distribution pattern calculated for [(Tp^{Me2})Fe(mandelate)]$^+$ (Fig. S13, ESI). The GC-MS of the methyl ester of mandelic acid shows a molecular ion peak at *m/z* = 166. When the reaction is carried out with $^{18}O_2$, the ion peaks are shifted to 168 (50% ^{18}O atom) and 170 (45% ^{18}O atom) (Fig. 4). Labeling experiments clearly indicate that both the oxygen atoms in mandelic acid are derived from dioxygen. A mixed labeling experiment with O_2 and H_2O^{18} reveals partial incorporation of single labeled oxygen into mandelic acid (Fig. S14, ESI).

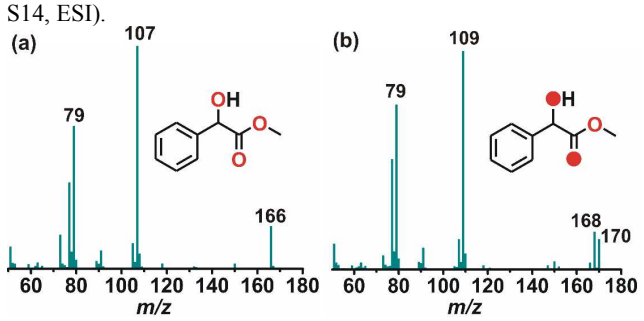

Fig. 4 GC-mass spectra of the methyl ester of mandelic acid. Mandelic acid is formed in the reaction of **1** with (a) $^{16}O_2$ and (b) with $^{18}O_2$.

In the time-dependent ^{1}H NMR spectra of the reaction of **1** with O_2, a transient complex appears after 5 min, which completely decays after 25 min (Fig. S7, ESI). The ^{1}H NMR spectrum of the transient species is similar to that of an indepedently prepared iron(II)-mandelate complex [(Tp^{Ph,Me})Fe^{II}(mandelate)(MeOH)](**3**) (Experimental Section and Fig. S15, ESI). The colorless solution of **3** in acetonitrile turns light green over a period of 45 min and the ESI-MS of the oxidized solution exhibits ion peaks with the isotope distribution patterns calculated for [(Tp^{Ph,Me*})Fe]$^+$, and {[(Tp^{Ph,Me*})Fe(OBz)] + H}$^+$ (Figs. S16 and S17, ESI). At end of the reaction about 19% benzoic acid, 59% benzaldehyde and 5% benzyl alcohol are formed (Fig. S18, ESI). Importantly, the iron(II)-phenylacetate complex **2** does not afford mandelic acid or benzaldehyde or benzoic acid upon exposure to O_2. An iron(II)-mandelate complex of Tp^{Ph2} ligand has been reported to form benzaldehyde, benzoic acid and benzyl alcohol in the reaction with O_2.[30] A nucleophilic iron-oxygen oxidant generated after decarboxylation of mandelate has been implicated to carry out the oxidation of benzaldehyde to benzoic acid. Benzyl alcohol is formed through Cannizzaro reaction of benzaldehyde.[30] These experimental results clearly establish that benzaldehyde (and benzoic acid) is derived from mandelate and leaves no doubt about the intermediacy of an iron(II)-mandelate complex in the decarboxylation of complex **1**. As observed in complex **3**, ligand hydroxylation is also observed upon longer exposure of the final oxidized solution of **1** (Fig. S19, ESI). Thus, on the basis of total yield of benzaldehyde and benzoic acid, formation of about 41% mandelic acid is estimated for **1** (Scheme S1). The formation of mandelic acid through oxidative decarboxylation of phenylpyruvate with the incorporation of both the oxygen atoms of O_2 functionally mimics the reaction catalyzed by hydroxymandelate synthase (HMS).

As no iron-oxygen intermediate could be observed for spectroscopic characterization, external substrates were used to intercept the active iron-oxygen species involved in the reaction pathway (Scheme S2).[31] In the reaction of **1** with 10 eqv thioanisole, 25% thioanisole oxide is obtained as the only product (Fig. S20, ESI). However, with reduced amount of thioanisole (2 eqv), a mixture of sulfoxide and sulfone is formed. With dimethyl sulfoxide as a substrate, 35% dimethyl sulfone is obtained (Fig. S21, ESI). The reaction of **1** with O_2 affords 30% fluorenone and 32% anthracene from fluorene and 9,10-dihydroanthracene, respectively (Fig. S22-S23, ESI). While cyclohexene yields *cis*-cyclohexane-1,2-diol (5%), a mixture *cis*-cyclooctane-1,2-diol (5%) and cyclooctene oxide (5%) are obtained from cyclooctene (Figs. S24-S27, ESI). With 1-octene, 33% octane-1,2-diol is observed (Fig. S28, ESI). Reaction of **1** with $^{18}O_2$ indicates the incorporation of both the labeled oxygen into octane-1,2-diol and a single labeled oxygen into thioanisole oxide (Figs. S29-S30, ESI). Additionally, a mixed labeling experiment with $^{16}O_2$ and H_2O^{18} shows no incorporation of labeled oxygen from ^{18}O enriched water into the products. In the interception experiments with thioanisole or 1-octene, the yield of benzoic acid is decreased but the total amount of benzaldehyde and benzoic acid remains constant. Also, the yield of phenylacetic acid remains unaltered in the presence of these substrates. Moreover, the yields of substrate-derived products are found to be less than 40%. All these results clearly illustrate that a metal-based nucleophilic oxidant derived from in situ generated iron(II)-mandelate is mainly responsible for substrate oxidation.

Taking into account all the results, a mechanistic proposal is put forward (Scheme 2). In the first step, iron(II)-phenylpyruvate complex undergoes oxidative decarboxylation to generate an iron(IV)-oxo species as proposed for α-keto acid-dependent enzymes. Since nonheme iron(IV)-oxo complexes have been reported to hydroxylate aliphatic C-H bonds,[32] the iron(IV)-oxo species in the present system hydroxylates the benzylic carbon of the coordinated PAA to form an iron(II)-mandelate species. The iron(II)-mandelate rapidly reacts with another molecule of O_2 in the same manner as reported for iron(II)-α-hydroxy acid complexes of Tp^{Ph2} ligand.[27, 30] Initially an iron(III)–superoxide complex is formed that abstracts the hydrogen atom from the -OH group of mandelate to form an iron(III)–hydroperoxide species

View Article Online
DOI: 10.1039/C5CC01652E

and a bound mandelate oxyl radical. The latter spontaneously decomposes, resulting in C-C bond cleavage to form benzaldehyde and CO_2 with concomitant reduction of iron(III) to iron(II). The side-on bound iron(II)–hydroperoxide intermediate thus formed carries out the oxidation of various substrates including *cis*-dihydroxylation of alkenes.

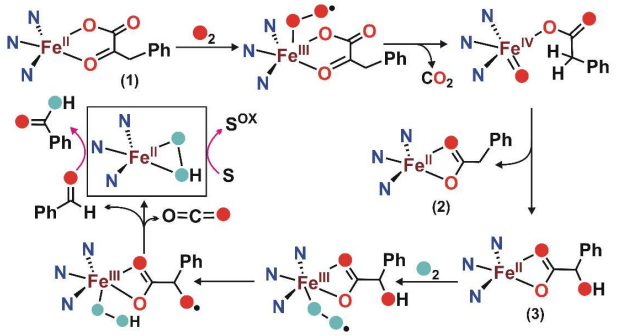

Scheme 2 Mechanistic proposal of two consecutive oxidative decarboxylations of phenylpyruvic acid on iron(II) complexes.

In conclusion, we have isolated and characterized two biomimetic iron(II)-phenylpyruvate complexes supported by tris(pyrazolyl)borate ligands. The complexes react with O_2 to undergo oxidative decarboxylation to form phenylacetic acid, benzaldehyde and benzoic acid. Mechanistic studies reveal the involvement of a putative iron(IV)-oxo oxidant in the oxidation of phenylacetate to mandelate. The iron(II)-mandelate complex, generated in situ, further reacts with O_2 to form benzaldehyde and benzoic acid. The formation of mandelic acid from the iron(II)-phenylpyruvate complex represents the first functional model of HMS and the first step of CloR through hydroxylation at the benzylic position of PAA. The conversion of in situ formed mandelate to benzaldehyde and benzoic acid represents the functional model mimicking the second step of CloR. The results described herein demonstrate the role of steric and electronic factors of the ligand in directing the specific oxygen-dependent transformation reaction.

TKP acknowledges the DST, India (Project: SR/S1/IC-51/2010) for financial support. DS thanks CSIR, India, and SB thanks DST(INSPIRE) for research fellowships.

Notes and references

[a]*Department of Inorganic Chemistry, Indian Association for the Cultivation of Science, 2A&2B Raja S. C. Mullick Road, Jadavpur, Kolkata-700032, India. Fax: +91-33-2473-2805; Tel: +91-33-2473-4971; E-mail: ictkp@iacs.res.in*

† Electronic Supplementary Information (ESI) available: Experimental procedure, spectral and crystalographic data. CCDC-1013639. See DOI: 10.1039/b000000x/

1. R. P. Hausinger, *Crit. Rev. Biochem. Mol. Biol.*, 2004, **39**, 21-68.
2. V. Purpero and G. R. Moran, *J. Biol. Inorg. Chem.*, 2007, **12**, 587-601.
3. C. J. Schofield and Z. Zhang, *Curr. Op. Struct. Biol.*, 1999, **9**, 722-731.
4. M. Costas, M. P. Mehn, M. P. Jensen and L. Que, Jr., *Chem. Rev.*, 2004, **104**, 939-986.
5. P. He and G. R. Moran, *Curr. Opin. Chem. Biol.*, 2009, **13**, 443-450.
6. P. He, J. A. Conrad and G. R. Moran, *Biochemistry*, 2010, **49**, 1998-2007.
7. J. Brownlee, P. He, G. R. Moran and D. H. T. Harrison, *Biochemistry*, 2008, **47**, 2002-2013.
8. K. Johnson-Winters, V. M. Purpero, M. Kavana, T. Nelson and G. R. Moran, *Biochemistry*, 2003, **42**, 2072-2080.
9. G. R. Moran, *Arch. Biochem. Biophys.*, 2014, **544**, 58-68.
10. O. W. Choroba, D. H. Williams and J. B. Spencer, *J. Am. Chem. Soc.*, 2000, **122**, 5389-5390.
11. C. M. L. Di Giuro, C. Konstantinovics, U. Rinner, C. Nowikow, E. Leitner and G. D. Straganz, *PLOS ONE*, 2013, **8**, e68932.
12. S. M. Pratter, C. Konstantinovics, C. M. L. Di Giuro, E. Leitner, D. Kumar, S. P. de Visser, G. Grogan and G. D. Straganz, *Angew. Chem. Int. Ed.*, 2013, **52**, 9677-9681.
13. J. M. Brownlee, K. Johnson-Winters, D. H. T. Harrison and G. R. Moran, *Biochemistry*, 2004, **43**, 6370-6377.
14. C. Krebs, D. G. Fujimori, C. T. Walsh and J. M. Bollinger, Jr., *Acc. Chem. Res.*, 2007, **40**, 484-492.
15. A. Wójcik, E. Broclawik, P. E. M. Siegbahn and T. Borowski, *Biochemistry*, 2012, **51**, 9570-9580.
16. M. Neidig, A. Decker, O. Choroba, F. Huang, M. Kavana, G. Moran, J. Spencer and E. I. Solomon, *Proc. Natl. Acad. Sci. U. S. A.,* 2006, **103**, 12966-12973.
17. T. Borowski, A. Bassan and P. E. M. Siegbahn, *Biochemistry*, 2004, **43**, 12331-12342.
18. F. Pojer, R. Kahlich, B. Kammerer, S.-M. Li and L. Heide, *J. Biol. Chem.*, 2003, **278**, 30661-30668.
19. T. K. Paine and L. Que, Jr., *Struct. Bond.*, 2014, **160**, 39-56.
20. M. P. Mehn, K. Fujisawa, E. L. Hegg and L. Que, Jr., *J. Am. Chem. Soc.*, 2003, **125**, 7828-7842.
21. P. C. A. Bruijnincx, G. van Koten and R. J. M. K. Gebbink, *Chem. Soc. Rev.*, 2008, **37**, 2716-2744.
22. T. K. Paine, S. Paria and L. Que, Jr., *Chem. Commun.*, 2010, **46**, 1830-1832.
23. T. K. Paine, H. Zheng and L. Que, Jr., *Inorg. Chem.*, 2005, **44**, 474-476.
24. T. K. Paine, J. England and L. Que, Jr., *Chem. Eur. J.*, 2007, **13**, 6073-6081.
25. N. Burzlaff, *Angew. Chem. Int. Ed.*, 2009, **48**, 5580-5582.
26. S. Paria, P. Halder and T. K. Paine, *Angew. Chem. Int. Ed.*, 2012, **51**, 6195-6199.
27. S. Paria, L. Que, Jr. and T. K. Paine, *Angew. Chem. Int. Ed.*, 2011, **50**, 11129-11132.
28. M. Sallmann, I. Siewert, L. Fohlmeister, C. Limberg and C. Knispel, *Angew. Chem. Int. Ed.*, 2012, **51**, 2234-2237.
29. A. W. Addison, T. N. Rao, J. Reedijk, J. van Rijn and G. C. Verschoor, *J. Chem. Soc., Dalton Trans.*, 1984, 1349-1356.
30. S. Paria, S. Chatterjee and T. K. Paine, *Inorg. Chem.*, 2014, **53**, 2810-2821.
31. A. Mukherjee, M. Martinho, E. L. Bominaar, E. Münck and L. Que, Jr., *Angew. Chem. Int. Ed.*, 2009, **48**, 1780-1783.
32. W. Nam, *Acc. Chem. Res.*, 2007, **40**, 522-531.